Synthesis and Characterization of a Stable *trans*-Dioxo Tungsten(IV) Complex and Series of Mono-Oxo Molybdenum(IV) and Tungsten(IV) Complexes. Structural and Electronic Effects of π-Bonding in *trans*-$[M(O)(X)(dppe)_2]^{+/0}$ Systems

Jesper Bendix*,† and Anders Bøgevig‡

Department of Inorganic Chemistry and Centre for Crystallographic Studies, University of Copenhagen, Universitetsparken 5, DK-2100 Copenhagen, Denmark

Received March 25, 1998

trans-$[W(O)(F)(dppe)_2](BF_4)$ (dppe = $Ph_2PCH_2CH_2PPh_2$, 1,2-bis(diphenylphosphino)ethane) (**10**) has been synthesized. From this, the neutral *trans*-$[W(O)_2(dppe)_2]\cdot 2CH_3OH$ (**11**) was prepared by a hydrolysis and deprotonation reaction with Et_4NOH in methanol/water. Together with the analogous molybdenum compound (**2**) this compound afforded by substitution under acid conditions salts of *trans*-$[M(O)(X)(dppe)_2]^+$ ions (M = Mo, W; X = OH, OCH_3, Cl, Br, I, NCS) and *trans*-$[Mo(O)(N_3)(dppe)_2](CF_3SO_3)$ (**9**). All the compounds have low-spin d^2 electronic configuration. The compounds were characterized by $^{31}P\{^1H\}$ NMR, positive FAB-ionization mass spectrometry, UV−vis spectroscopy, and vibrational spectroscopy. X-ray crystallographic studies were carried out on compounds **10**, **11**, *trans*-$[W(O)(OH)(dppe)_2](ClO_4)$ (**12**), and *trans*-$[W(O)(NCS)(dppe)_2](BPh_4)$ (**16**). The electronic spectra of the mono-oxo species are consistent with the lowest energy transitions being of $d_{xy} \rightarrow \{d_{zx}, d_{yz}\}$ character. No ligand-field transitions are observed for the dioxo tungsten complex. Identical π-spectrochemical series were found for the two metals. The shielding of the phosphorus nuclei determined by $^{31}P\{^1H\}$ NMR is significantly influenced by the nature of the axial ligands.

Introduction

Multiple bonding between transition metals and ligands has received much interest recently, fueled by its importance for atom-transfer reactions in catalysis and biochemistry.[1,2] Among the systems with multiple-bonding between metals and ligands a rich subclass of strongly tetragonally compressed *trans*-dioxo complexes of metal centers d^2 electronic configurations has developed. This class encompasses complexes of technetium(V),[3] rhenium(V),[4] ruthenium(VI),[5] and osmium(VI).[6] The photochemical and photophysical properties of these compounds have been the focus of much interest.[7] Contrary to these four metals, only very few molybdenum(IV) and tungsten(IV) dioxo complexes have been described. These are the *trans*-$[M(O)_2(CN)_4]^{4-}$ ions[8] and the matrix-isolated *trans*-$[M(O)_2(CO)_4]$ (M = Mo, W) complexes.[9]

Recently, Cotton *et al.*[10,11] and we[12] have augmented these with compounds of the type *trans*-$[Mo(O)_2(PP)_2]\cdot 2$(solvate) where PP represents one of the two bidentate phosphine ligands, dppe ($Ph_2PCH_2CH_2PPh_2$, 1,2-bis(diphenylphosphino)ethane) or dppee ($Ph_2PCH{=}CHPPh_2$, *cis*-1,2-bis(diphenylphosphino)ethylene). Analogous tungsten(IV) complexes have, however, not been described despite the facts that *trans*-$[Re(O)_2(dppe)_2](ReO_4)$ has been known for 30 years[13] and that similar complexes of the heavier calcogenides (*trans*-$[W(Q)_2(P(CH_3)_3)_4]$, Q = S, Se, Te) were described in a pioneering work by Rabinovich and Parkin.[14]

Some examples of related cationic complexes of the type *trans*-$[M(O)(X)(dppe)_2]^+$ (M = Mo, W) have been reported: *trans*-$[Mo(O)(Cl)(dppe)_2]^+$,[15] *trans*-$[W(O)(Cl)(dppe)_2]^+$,[16] *trans*-

† Department of Inorganic Chemistry.
‡ Centre for Crystallographic Studies.

(1) Nugent, W. A.; Mayer, J. M. *Metal−Ligand Multiple Bonds*; Wiley: New York, 1988.
(2) Holm, R. H. *Chem. Rev.* **1987**, *87*, 1401.
(3) (a) Trop, H. S.; Jones, A. G.; Davison, A. *Inorg. Chem.* **1980**, *19*, 1993. (b) Kastner, M. E.; Lindsay, M. J.; Clarke, M. J. *Inorg. Chem.* **1982**, *21*, 2037. (c) Fackler, P. H.; Lindsay, M. J.; Clarke, M. J. *Inorg. Chem. Acta* **1985**, *109*, 39. (d) Vanderheyden, J.-L.; Ketring, A. R.; Libson, K.; Heeg, M. J.; Roecker, L.; Motz, P.; Whittle, R.; Elder, R. C.; Deutsch, E. *Inorg. Chem.* **1984**, *23*, 3184.
(4) (a) Winkler, J. R.; Gray, H. B. *Inorg. Chem.* **1985**, *24*, 346. (b) Winkler, J. R.; Gray, H. B. *J. Am. Chem. Soc.* **1983**, *105*, 1373. (c) Pipes, D. W.; Meyer, T. J. *Inorg. Chem.* **1986**, *25*, 3256. (d) Yam, V. W−W.; Tam, K.-K.; Cheng, M.-C.; Peng, S.-M.; Wang, Y. *J. Chem. Soc., Dalton Trans.* **1992**, 1727.
(5) (a) Griffith, W. P.; Pawson, D. *J. Chem. Soc., Dalton Trans.* **1973**, 1315. (b) Tokita, Y.; Yamaguchi, K.; Watanabe, Y.; Morishima, I. *Inorg. Chem.* **1993**, *32*, 329. (c) Hepworth, M. A.; Robinson, P. L. *Inorg. Nucl. Chem.* **1957**, *4*, 24. (d) Mak, T. C. W.; Che, C.-M.; Wong, K.-Y. *J. Chem. Soc., Chem. Commun.* **1985**, 986.
(6) (a) Che, C.-M.; Yam, V. W−W.; Cho, K.-C.; Gray, H. B. *J. Chem. Soc., Chem. Commun.* **1987**, 948. (b) Malin, J. M.; Schlemper, E. O.; Murmann, R. K. *Inorg. Chem.* **1977**, *16*, 615. (c) Phillips, F. L.; Skarpski, A. *Acta Crystallogr.* **1975**, *B31*, 1814. (d) Kruse, F. H. *Acta Crystallogr.* **1961**, *14*, 1035.
(7) (a) Che, C. M.; Yam, V. W. W.; Cho, K. C.; Gray, H. B. *J. Chem. Soc., Chem. Commun.* **1987**. 948. (b) Yam, V. W. W.; Che, C. M. *Coord. Chem. Rev.* **1990**, *97*, 93. (c) Lam, H. W.; Chin, K. F.; Che, C. M.; Wang, R. J.; Mak, T. C. W. *Inorg. Chim. Acta* **1993**, *204*, 133. (d) Winkler, J. R.; Gray, H. B. *Inorg. Chem.* **1985**, *24*, 346.
(8) (a) Day, V. W.; Hoard, J. L. *J. Am. Chem. Soc.* **1968**, *90*, 3374. (b) Lippard, S. J.; Russ, B. J. *Inorg. Chem.* **1967**, *6*, 1943. (c) Samotus, A.; Dudek, M.; Kanas, A. *J. Inorg. Nucl. Chem.* **1975**, *37*, 943.
(9) Crayston, J. A.; Almond, M. J.; Downs, A. J.; Poliakoff, M.; Turner, J. J. *Inorg. Chem.* **1984**, *23*, 3051.
(10) Cotton, F. A.; Feng, X. *Inorg. Chem.* **1996**, *35*, 4921.
(11) Cotton, F. A.; Schmid, G. *Inorg. Chem.* **1997**, *36*, 2267.
(12) Bendix, J.; Birkedal, H.; Bøgevig, A. *Inorg. Chem.* **1997**, *36*, 2702.
(13) Freni, M.; Giusto, D.; Romiti, P. *Gazz. Chim. Ital.* **1967**, *97*, 833.
(14) Rabinowich, D.; Parkin, G. *Inorg. Chem.* **1995**, *34*, 6341.
(15) (a) Bishop, M. W.; Chatt, J.; Dilworth, J. R.; Hursthouse, M. B.; Motevalli, M. *J. Chem. Soc., Dalton Trans.* **1979**, 1603. (b) Adam, V. C.; Gregory. U. A.; Kilbourn, B. T. *J. Chem. Soc., Chem. Commun.* **1970**, 1400.

10.1021/ic980342u CCC: $15.00
Published on Web 10/24/1998

$[Mo(O)(F)(dppe)_2]^+$,[17] and *trans*-$[Mo(O)(OCH_3)(dppe)_2]^+$.[18] However, only the first of these complexes was a result of an intended synthesis with a reported yield. In addition to these four complexes also *trans*-$[Mo(O)(OH)(dppe)_2]^+$ [19] has been claimed, but this result has been shown[12] to be a misinterpretation and the complex actually described to be *trans*-$[Mo(O)(F)(dppe)_2]^+$.

Here we describe the synthesis of *trans*-$[W(O)(F)(dppe)_2](BF_4)$ (**10**) and therefrom *trans*-$[W(O)_2(dppe)_2]\cdot 2CH_3OH$ (**11**). We further describe the rational synthesis of the two series of complexes: *trans*-$[M(O)(X)(dppe)_2]^+$ (M = W; OH (**12**), Cl (**13**), Br (**14**), I (**15**), NCS (**16**), OCH_3 (**17**), and M = Mo; X = OH (**3**), Cl (**4**), Br (**5**), I (**6**), NCS (**7**), OCH_3 (**8**), and N_3 (**9**)) utilizing the respective *trans*-dioxo complexes as versatile starting materials. The spectral and structural variations within and between these series are discussed.

Experimental Section

General Procedures. dppe and triphenylphosphine were purchased (Strem) and used without further purification. Aqueous solutions of HBF_4 (Fluka), $Pb(BF_4)_2$ (Riedel-de Haën), and Et_4NOH (Fluka) were purchased and used as received. CF_3SO_3H was purchased (3M-Company) and purified by distillation of the mono hydrate. Trimethylsilyl azide was purchased (Fluka) and used as received. *trans*-$W(PPh_3)_2Cl_4$[20] and $Na_3[Mo(HCOO)_6]$[21] were prepared by literature procedures. The syntheses of *trans*-$[Mo(O)(F)(dppe)_2](BF_4)$ (**1**), *trans*-$[Mo(O)_2(dppe)_2]\cdot 2CH_3OH$ (**2**), and *trans*-$[Mo(O)(OH)(dppe)_2](ClO_4)$ (**3**) have been outlined in a previous communication;[12] the details are given here. Fast atom bombardment (FAB) mass spectra (Xe ions, accelerated by 6 kV) were recorded on a Jeol JMS-HX/HX110A tandem mass spectrometer (positive ion detection. Matrix: *m*-nitrobenzyl alcohol (*m*-NBA) or glycerol). In all cases only peaks which could be rationalized as fragments of the molecular ions were observed. Good agreement between calculated and observed isotope patterns was found for all important peaks. UV−vis spectra were recorded on a Perkin-Elmer, Lambda 17 spectrometer. ^{31}P and ^{19}F NMR spectra were recorded on a Varian UNITY 400 spectrometer operating at 161.90 and 376.28 MHz, respectively. All spectra were recorded in $CDCl_3$. ^{31}P NMR spectra were recorded with H_3PO_4 as external reference and ^{19}F NMR spectra with $CF_3C_6H_5$ ($\delta = -63.75$ ppm vs $CFCl_3$) as external reference. The quoted ^{19}F chemical shifts are relative to $CFCl_3$. Infrared and Raman ($\lambda = 1064$ nm) spectra were recorded on solid samples (KBr disks) on a Perkin-Elmer 2000 FT-IR/FT-NIR Raman spectrometer. Melting points were measured on a Büchi melting point apparatus. Elemental analyses were made at the Microanalytical Laboratory at the Department of Chemistry, University of Copenhagen.

Safety Note. *Azide complexes and perchlorate salts of metal complexes are potentially explosive. Only in small amounts of material should be prepared and these should be handled with great caution. The described perchlorates explode when heated in the solid state.*

Synthesis of *trans*-$[Mo(O)(F)(dppe)_2](BF_4)$ (1). $Na_3[Mo(HCOO)_6]$ (100 mg, 0.23 mmol) and dppe (180 mg, 0.45 mmol) were refluxed for 3 h in a mixture of 96% ethanol (18 mL), 40% aqueous HBF_4 (1 mL, 8 mmol), and water (1 mL). From the resulting dark red solution pink crystals precipitated upon cooling in ice. The precipitate was washed with a 1:1 mixture of methanol/diethyl ether followed by diethyl ether. Yield 170 mg (74%). Anal. Calcd for $MoOP_4F_5BC_{52}H_{48}$: C, 61.56; H, 4.77. Found: C, 61.62; H, 4.82. Mp 275−285 °C (dec). FAB-MS (glycerol matrix): *m*/*z* 929 (M^+, rel intensity 63%), 531 ((M − dppe)$^+$, rel intensity 100%).

Synthesis of *trans*-$[Mo(O)_2(dppe)_2]\cdot 2CH_3OH$ (2). **1** (200 mg, 0.20 mmol) was added to a solution of 15 mL of acetone and 10 mL of methanol. When the pink *trans*-$[Mo(O)(F)(dppe)_2](BF)_4$ had completely dissolved, the solution was filtered and tetraethylammonium hydroxide (5 drops of 40% aqueous solution, 0.7 mmol) was layered with the solution. The reaction mixture was cooled to 5 °C. During several hours yellow crystals grew. The compound does not survive for more than 1 day under these conditions. If good quality crystals are not needed, addition of 3−5 times larger amount of base and immediate mixing will produce a yellow microcrystalline powder. Yield 170 mg (87%). Anal. Calcd for $MoO_4P_4C_{54}H_{56}$: C, 65.59; H, 5.71. Found: C, 64.71; H, 5.79. Mp 131−133 °C (dec). FAB-MS (*m*-NBA matrix): *m*/*z* 927 ((M + H)$^+$, rel intensity 17%), 529 ((M + H − dppe)$^+$, rel intensity 100%). Adducts with water, ethanol, or 2-propanol can be made in similar yields by substituting these solvents for the methanol above.

Synthesis of *trans*-$[Mo(O)(OH)(dppe)_2](ClO_4)$ (3). To a suspension of **2** (200 mg) in methanol (30 mL) was slowly added 1 M $HClO_4$ (30 mL). After addition of the first 5 drops a clear orange solution resulted. Upon addition of the remaining $HClO_4$ the compound crystallized as yellow-orange plates. The yield was quantitative (200 mg). Anal. Calcd for $MoO_6P_4ClC_{52}H_{49}$: C, 60.92; H, 4.82; Cl, 3.46. Found: C, 59.94; H, 4.65; Cl, 3.53. Mp 170 °C (expl.). FAB-MS (*m*-NBA matrix): *m*/*z* 927 (M^+, rel intensity 91%), 529 ((M − dppe)$^+$, rel intensity 67%).

Synthesis of *trans*-$[Mo(O)(Cl)(dppe)_2]Cl\cdot 2H_2O$ (4). To a suspension of **2** (100 mg, 0.101 mmol) in methanol (15 mL) was added 0.2 mL of 1 M aqueous HCl, the solution was filtered and added 1 M HCl (10 mL). The blue solution deposits 90 mg (88%) of blue flaky crystals. Anal. Calcd for $MoO_2Cl_2P_4C_{52}H_{50}$: C, 61.49; H, 5.16; Cl, 6.98. Found: C, 59.07; H, 5.06; Cl, 6.81. Mp 147−151 °C (dec). FAB-MS (*m*-NBA matrix): *m*/*z* 945 (M^+, rel intensity 100%), 547 ((M − dppe)$^+$, rel intensity 70%).

Synthesis of *trans*-$[Mo(O)(Br)(dppe)_2]Br\cdot 2H_2O$ (5). This compound was synthesized in the same way as the chloro-complex, substituting HBr for HCl. Yield 82%. Anal. Calcd for $MoO_2Br_2P_4C_{52}H_{50}$: C, 56.54; H, 4.75; Br, 14.47. Found: C, 55.14; H, 4.69; Br, 14.31. Mp ca. 131 °C (dec). FAB-MS (*m*-NBA matrix): *m*/*z* 989 (M^+, rel intensity 100%), 591 ((M − dppe)$^+$, rel intensity 72%).

Synthesis of *trans*-$[Mo(O)(I)(dppe)_2](BPh_4)$ (6). **2** (150 mg, 0.152 mmol), NH_4I (1.35 g, 13.1 mmol), and 0.75 mL of aqueous CF_3SO_3H was refluxed in 2-propanol (15 mL) for 1 h. The green solution was cooled to 20 °C and diluted with methanol (45 mL). Slow addition of $NaBPh_4$ (400 mg, 1.17 mmol) in methanol (30 mL) afforded green crystals which were washed with methanol (4×) and diethyl ether (2×). Yield 128 mg (62%). Anal. Calcd for $MoOIBP_4C_{76}H_{68}$: C, 67.37; H, 5.06; I, 9.37. Found: C, 67.04; H, 5.00; I, 9.87. Mp 200−208 °C (dec). FAB-MS (*m*-NBA matrix): *m*/*z* 1036 (M^+, rel intensity 22%), 638 ((M − dppe)$^+$, rel intensity 15%).

Synthesis of *trans*-$[Mo(O)(NCS)(dppe)_2](BPh_4)$ (7). **2** (160 mg, 0.162 mmol) and NH_4NCS (1.00 g, 13.1 mmol) was refluxed in 2-propanol (12 mL) for 0.5 h. The green solution was cooled to 20 °C and diluted with methanol (25 mL). Slow addition of $NaBPh_4$ (480 mg, 1.40 mmol) in methanol (45 mL) afforded blue solid. The raw product was dissolved in acetone (12 mL). To the filtered solution was slowly added 0.50 g $NaBPh_4$ in methanol (40 mL). Yield 110 mg (53%) of blue-violet needles. Anal. Calcd for $MoONSBP_4C_{77}H_{68}$: C, 71.91; H, 5.33; N, 1.09. Found: C, 71.62; H, 5.17; N, 1.05. Mp 200−206 °C (dec). FAB-MS (*m*-NBA matrix): *m*/*z* 968 (M^+, rel intensity 24%).

Synthesis of *trans*-$[Mo(O)(OCH_3)(dppe)_2](CF_3SO_3)$ (8). To a suspension of **2** (150 mg, 0.152 mmol) in methanol (15 mL) was added neat CF_3SO_3H (0.25 mL). The solution was refluxed for 2 h, cooled to 0 °C, and 10 mL of 2 M aqueous CF_3SO_3H was added. The product was washed with cold methanol (1×) and diethyl ether (2×). Yield 125 mg (76%) of yellow orange crystals. Anal. Calcd for $MoO_5P_4C_{54}H_{51}SF_3$: C, 59.57; H, 4.72. Found: C, 57.93; H, 4.67. Mp ca. 190 °C (dec). FAB-MS (*m*-NBA matrix): *m*/*z* 941 (M^+, rel intensity 100%, 543 (M − dppe)$^+$, rel intensity 95%).

(16) Cotton, F. A.; Mandal, S. K. *Eur. J. Solid State Inorg. Chem.* **1991**, *28*, 775.
(17) Morris, R. H.; Sawyer, J. F.; Schweitzer, C. T.; Sella, A. *Organometallics* **1989**, *8*, 2099.
(18) Adachi, T.; Hughes, D. L.; Ibrahim, S. K.; Okamoto, S.; Pickett, C. J.; Yabanouchi, N.; Youshida., T. *J. Chem. Soc., Chem. Commun.* **1995**, 1081.
(19) Churchill, M. R.; Rotella, F. J. *Inorg. Chem.* **1978**, *17*, 668.
(20) Butcher, A. V.; Chatt, J.; Leigh, G. J.; Richards, R. L. *J. Chem. Soc., Dalton Trans.* **1972**, 1064.
(21) Brorson, M.; Schäffer, C. E. *Acta Chem. Scand.* **1986**, *A 40*, 358.

Table 1. Crystallographic Data of Complexes

	10	**11**	**12**	**16**
empirical formula	$C_{52}H_{48}BF_5OP_4W$	$C_{54}H_{56}O_4P_4W$	$C_{52}H_{49}ClO_6P_4W$	$C_{77}H_{68}BNOP_4SW$
fw (g/mol)	1102.44	1076.72	1113.09	1373.92
temp (K)	122(2)	122(2)	122(2)	122(2)
wavelength (Å)	0.710 73	0.710 73	0.710 73	0.710 73
space group	*Cc* (No. 9)	$P\bar{1}$ (No. 2)	$P2_1/n$ (No. 14)	$P\bar{1}$ (No. 2)
unit cell dimensions				
a (Å)	9.814(5)	9.464(2)	16.864(3)	13.8122(3)
b (Å)	22.472(3)	11.429(2)	16.639(4)	19.0123(4)
c (Å)	21.1029(17)	13.126(3)	17.114(4)	24.9475(5)
α (deg)	−	110.86(2)	−	92.5320(10)
β (deg)	92.522(17)	99.05(2)	102.256(18)	98.6970(10)
γ (deg)	−	110.24(2)	−	93.7920(10)
V (Å^3)	4649(2)	1179.4(5)	4692.5(18)	6452.0(2)
Z	4	1	4	4
ρ_{calc} (g/cm^3)	1.575	1.516	1.576	1.414
μ (cm^{-1})	26.81	26.31	27.06	19.69
R1 [$I > 2\sigma(I)$][a]	0.0306	0.0173	0.0278	0.0698
wR2 [$I > 2\sigma(I)$][a]	0.0620	0.0433	0.0587	0.1638

[a] $R1 = \sum||F_o| - |F_c||/\sum|F_o|$; $wR2 = [\sum\{w(|F_o|^2 - |F_c|^2)^2\}/\sum\{w(|F_o|^2)^2\}]^{1/2}$.

Synthesis of *trans*-[Mo(O)(N$_3$)(dppe)$_2$](CF$_3$SO$_3$) (9). **2** (140 mg, 0.142 mmol) and $(CH_3)_3SiN_3$ (1 mL) were added to a mixture of 3 mL of methanol, 3 mL of acetone, and 2 mL of 2 M aqueous CF_3SO_3H. The clear solution was left in an open beaker for 24 h whereupon the deposited large blue needle-shaped crystals were collected and washed with methanol/diethyl ether (1:5) (3×) and diethyl ether (2×). Yield 120 mg (77%). Anal. Calcd for $MoO_4N_3P_4C_{53}H_{48}F_3S$: C, 57.88; H, 4.40; N, 3.82. Found: C, 56.68; H, 4.40; N, 3.50. Mp 212−215 °C (dec). FAB-MS (*m*-NBA matrix): *m*/*z* 952 (M^+, rel intensity 100%), 526 ((M − dppe − 2N)$^+$, rel intensity 15%), 924 ((M − 2N)$^+$, rel intensity 10%).

Synthesis of *trans*-[W(O)(F)(dppe)$_2$](BF$_4$) (10). *trans*-$W(PPh_3)_2Cl_4$ (2.55 g, 3.00 mmol) and dppe (3.10 g, 7.78 mmol) were suspended in a degassed mixture of 175 mL of 2-propanol, 25 mL of 50% aqueous HBF_4, and 12 mL of 50% aqueous $Pb(BF_4)_2$. The mixture was refluxed under N_2 for 16 h. After cooling the solids were filtered off, washed with water and diethyl ether, and then extracted with 200 mL of hot acetone. To the cooled extract was slowly added 200 mL of 0.4 M aqueous HBF_4. Yield 1.76 g (53%) of flesh-colored needles. Anal. Calcd for $WOP_4F_5BC_{52}H_{48}$: C, 56.65; H, 4.39. Found: C, 56.69; H, 4.44. Mp 285−290 °C dec. FAB-MS (glycerol matrix): *m*/*z* 1015 (M^+, rel intensity 100%), 617 ((M − dppe)$^+$, rel intensity 31%).

Synthesis of *trans*-[W(O)$_2$(dppe)$_2$]·2CH$_3$OH (11). **10** (1.10 g, 1.00 mmol) was dissolved in a mixture of 110 mL of acetone and 70 mL of methanol. To the filtered solution was added 12 mL of 40% aqueous NEt_4OH solution, and the reaction mixture was heated to 55 °C for 2 h. After cooling to room temperature, 0.99 g (92%) of bright yellow microcrystals was collected by filtration and washed with diethyl ether. Anal. Calcd for $WO_4P_4C_{54}H_{56}$: C, 60.23; H, 5.24. Found: C, 59.64; H, 5.15. Mp 121−122 °C (dec). FAB-MS (*m*-NBA matrix): *m*/*z* 1013 ((M + H)$^+$, rel intensity 90%), 615 ((M + H − dppe)$^+$, rel intensity 39%).

Synthesis of *trans*-[W(O)(OH)(dppe)$_2$](ClO$_4$) (12). To a suspension of **10** (150 mg, 0.139 mmol) in 10 mL of methanol cooled to 0 °C was slowly added 2.0 mL of 1 M $HClO_4$. The orange-yellow crystalline product was filtered off and washed with methanol (3×) and diethyl ether (2×). Yield 144 mg (93%). Anal. Calcd for $WO_6P_4ClC_{52}H_{49}$: C, 56.11; H, 4.44; Cl, 3.19. Found: C, 55.55; H, 4.38; Cl, 3.05. Mp 215 °C (expl.). FAB-MS (*m*-NBA matrix): *m*/*z* 1014 (M^+, rel intensity 100%), 616 ((M − dppe)$^+$, rel intensity 35%).

Synthesis of *trans*-[W(O)(Cl)(dppe)$_2$](ClO$_4$) (13). To a suspension of **10** (155 mg, 0.144 mmol) in 5.0 mL of acetone was added 2.0 mL of 12 M HCl. Immediately the dioxo compound dissolves and the solution turns red-violet. Addition of 1.5 mL of 1 M $HClO_4$, heating to give a clear solution, filtering, and cooling to 0 °C afforded purple crystals which were washed with ethanol (3×) and diethyl ether (2×). Yield 110 mg (68%). Anal. Calcd for $WO_5P_4Cl_2C_{52}H_{48}$: C, 55.13; H, 4.28; Cl, 6.27. Found: C, 54.81; H, 4.23; Cl, 6.31. Mp 198 °C (expl.). FAB-MS (*m*-NBA matrix): *m*/*z* 1032 (M^+, rel intensity 100%), 634 ((M − dppe)$^+$, rel intensity 68%).

Synthesis of *trans*-[W(O)(Br)(dppe)$_2$](BPh$_4$) (14). To a suspension of **10** (150 mg, 0.139 mmol) in 10 mL of acetone was added 0.8 mL of 48% aqueous HBr. The dioxo compound dissolves giving an orange solution which upon heating to 50 °C (5 min) turns violet. The solution was cooled to 0 °C and methanol (10 mL) added, followed by slow addition of $NaBPh_4$ (0.45 g, 1.32 mmol). The precipitate (80 mg, 41%) of blue-violet flaky crystals was filtered of and washed with methanol (3×). Anal. Calcd for $WOBrBP_4C_{76}H_{68}$: C, 65.40; H, 4.91; Br, 5.72. Found: C, 64.90; H, 4.90; Br, 5.70. Mp ca. 197 °C (dec). FAB-MS (*m*-NBA matrix): *m*/*z* 1078 (M^+, rel intensity 32%), 680 ((M − dppe)$^+$, rel intensity 9%).

Synthesis of *trans*-[W(O)(I)(dppe)$_2$](BPh$_4$) (15). **10** (250 mg, 0.232 mmol) and 3.2 g NaI was dissolved in 10 mL of neat HCOOH by heating to close to the boiling point for 5 min. The reaction mixture was cooled to 0 °C, and 10 mL of methanol was added to give a clear solution, followed by slow addition of a solution of 0.25 g $NaBPh_4$ in 10 mL of methanol. The precipitate was allowed to settle for 30 min and then filtered off and washed with methanol (3×). Yield 210 mg (63%). Anal. Calcd for $WOIBP_4C_{76}H_{68}$: C, 63.27; H, 4.75; I, 8.80. Found: C, 63.19; H, 4.70; I, 8.54. Mp ca. 201 °C (dec). FAB-MS (*m*-NBA matrix): *m*/*z* 1123 (M^+, rel intensity 12%), 725 ((M − dppe)$^+$, rel intensity 5%).

Synthesis of *trans*-[W(O)(*N*CS)(dppe)$_2$](BPh$_4$) (16). A solution of **10** (100 mg, 0.093 mmol) and NH_4SCN (0.62 g, 8.1 mmol) in 15 mL of methanol was refluxed for 2 h. To the resulting green solution was slowly added $NaBPh_4$ (0.30 g, 0.88 mmol) in methanol (10 mL). A purple crystalline precipitate was collected by filtration and washed with methanol (3×) and diethyl ether (2×). Anal. Calcd for $WONSBP_4C_{77}H_{68}$: C, 67.31; H, 4.99; N, 1.02. Found: C, 66.56; H, 5.01; N, 1.19. Mp 212−217 °C (dec). FAB-MS (*m*-NBA matrix): *m*/*z* 1054 (M^+, rel intensity 42%), 656 ((M − dppe)$^+$, rel intensity 13%).

Synthesis of *trans*-[W(O)(OCH$_3$)(dppe)$_2$]I (17). **10** (150 mg, 0.139 mmol) was dissolved in 5 mL of CH_3I. To the solution was added 5 mL of methanol, and the mixture was refluxed for 2 h, followed by stripping off the solvent on a rotatory evaporator. The yellow product was dissolved in 5 mL of methanol by heating. Cooling to 0 °C followed by slow addition of 3.5 mL of H_2O precipitated 123 mg (76%) of yellow-orange flakes. Anal. Calcd for $WO_2P_4IC_{53}H_{51}$: C, 55.13; H, 4.45; I, 10.99. Found: C, 54.39; H, 4.40; I, 11.38. Mp 224−226 °C (dec). FAB-MS (*m*-NBA matrix): *m*/*z* 1028 (M^+, rel intensity 13%), 630 ((M − dppe)$^+$, rel intensity 7%).

X-ray Crystallography. Crystal structure and refinement data for **10**, **11**, **12**, and **16** are summarized in Table 1. Details of the structure determinations are available in the Supporting Information. The disorder in **11** was modeled in a similar way as done for *trans*-[Mo(O)-

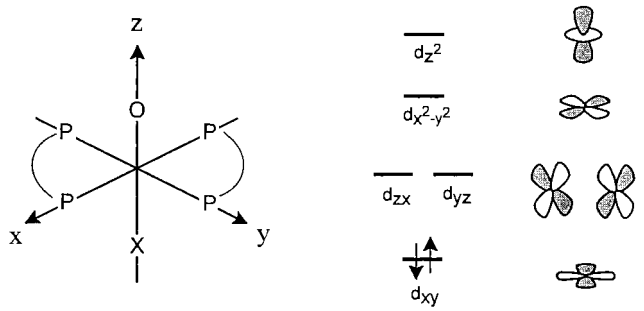

Figure 1. Coordinate system employed for the *trans*-$[M(O)(X)(dppe)_2]^{0/+}$ complexes. The orbital splitting pattern together with the orbital population in the resulting low-spin d^2 system are depicted on the right.

$(F)(Ph_2PCH{=}CHPPh_2)_2](BF_4)$ by Cotton *et al.*[22] The O, W, and F atoms were described by two fragments with opposite orientations: F−W−O and O−W−F. No restraints were made on the geometries or multiplicities of the two fragments, but common thermal parameters were imposed on the two fragments.

For **16** all of the non-hydrogen atoms were refined with anisotropic temperature factors, but all of the phenyl carbon atoms were restrained to be similar. The distance between neighboring carbon atoms in the phenyl groups was constrained to 1.39 Å. The distance from tungsten atoms to coordinating O and N atoms were restrained to be the same in both independent cations. The molecular structure diagrams were made with the ORTEP-II program.[23]

Results and Discussion

The rational synthesis and the characterization, by means of UV−vis, vibrational, and $^{31}P\{^1H\}$ NMR spectroscopies as well as by single-crystal X-ray diffraction of the two parallel series *trans*-$[W(O)(X)(dppe)_2]^+$, provides an unprecedented possibility for studying the variation of π-antibonding effects in similar systems.

For strongly tetragonally compressed octahedral complexes, like the ones in question, the orbital splitting scheme in Figure 1 is applicable. This orbital scheme was originally invoked by Jørgensen[24] and by Ballhausen and Gray[25] to explain the electronic structure of the vanadyl ion.

The low-spin d^2 electronic configuration of the *trans*-$[M(O)(X)(dppe)_2]^+$ was confirmed by the narrow-line unshifted ^1H, ^{13}C, and ^{31}P NMR spectra recorded on the complexes. Furthermore, the magnetic susceptibilities of the fluoro complexes **1** and **10** were measured and gave, when corrected for diamagnetism, a temperature independent (60−290 K) magnetic susceptibility (TIP) of around 110×10^{-6} cgsu, which corresponds to a room-temperature magnetic moment of 0.50 μ_B. This value is in the range expected for low-spin d^2 systems. Although several studies[26] report metal centers with this electronic configuration to be diamagnetic, complete configuration ligand-field calculations predict, irrespective of the magnitude of the spin−orbit coupling parameter, room-temperature magnetic moments of around 0.5 μ_B.[27]

Syntheses. The synthetic pathways to the molybdenum and tungsten series of complexes *trans*-$[M(O)(X)(dppe)_2]^+$ are outlined in Schemes 1 and 2, respectively. The generality of the approach of replacing one oxo ligand in the neutral *trans*-dioxo species with singly charged anions by substitution under acidic conditions is clearly demonstrated by the range of examples provided here. Yields between 40% and 90% from the easily accessible dioxo complexes make these routes the first general synthetically useful approach to this type of complexes. Compared with other solvents, dilute methanol solutions were found to give superior crystallinity and purity of the product in the cases where tetraphenylborate salts of the cations were isolated. However, for the iodo complexes heating with methanol resulted in contamination with the corresponding methoxy complexes. For these systems 2-propanol or formic acid were suitable reaction media in the syntheses.

Scheme 1. Schematic Representation of the Synthetic Routes to the Molybdenum Complexes and Labeling Scheme for These

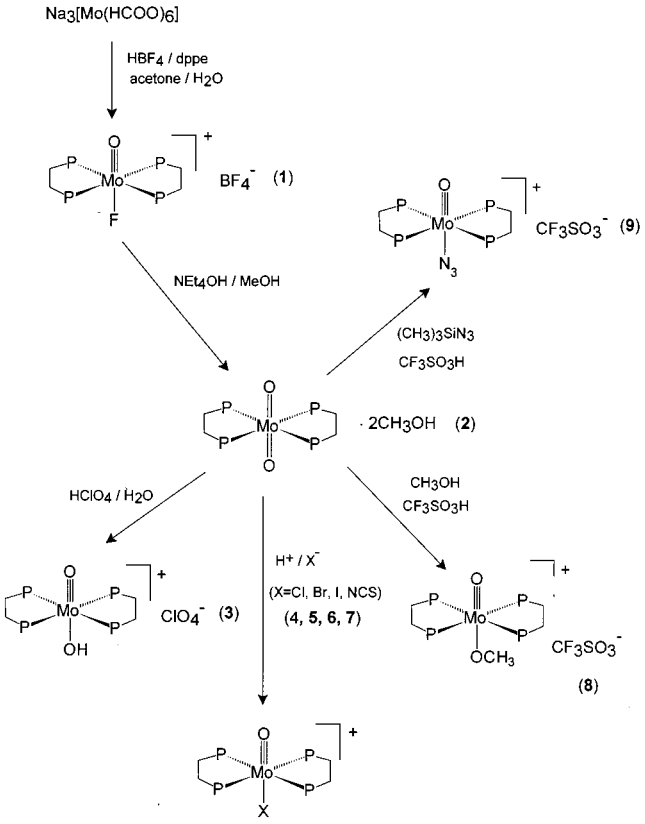

By letting the known high-spin tungsten(IV) compound *trans*-$WCl_4(PPh_3)_2$ react with dppe and $HBF_4/Pb(BF_4)_2$ in an acetone water mixture, flesh-colored **10** was obtained. Addition of a source of Pb^{2+} ions was found to be necessary to avoid contamination of the product with large amounts of *trans*-$[W(O)(Cl)(dppe)_2](BF_4)$. The possibility of BF_4^- acting as a fluoride source was also observed in the molybdenum chemistry.[12] The synthetic pathway to **11** by a substitution-deprotonation reaction of *trans*-$[W(O)(F)(dppe)_2]^+$ is similar to the route previously described for the molybdenum analogue.[12] This yellow compound is nearly insoluble in most solvents but like its molybdenum analogue it reacts smoothly with halogenated methanes.

The acid-catalyzed substitution reactions are likely to occur via the diprotonated *trans*-oxo-aqua complexes. We have not investigated this point quantitatively, but noted that the substitution rate increases with the concentration and strength of the added acid. A dissociative mechanism, with the *trans*-oxo aqua

(22) Cotton, F. A.; Eglin, J. L.; Wiesinger, K. J. *Inorg. Chim. Acta* **1992**, *195*, 11.
(23) Johnson, C. K. *ORTEP-II*; Report ORNL-5138; Oak Ridge National Laboratory, TN, 1976.
(24) Jørgensen, C. K. *Acta Chem. Scand.* **1957**, *11*, 73.
(25) (a) Ballhausen, C. J.; Gray, H. B. *Inorg. Chem.* **1962**, *1*, 111. (b) Winkler, J. R.; Gray, H. B. *Inorg. Chem.* **1985**, *24*, 346.
(26) (a) Novotny, M.; Lippard, S. J. *Inorg. Chem.* **1974**, *13*, 828. (b) Fackler, P. H.; Lindsay, M. J.; Clarke, M. J.; Kastner, M. E. *Inorg. Chim. Acta* **1985**, *109*, 39.
(27) Bendix, J. To be published.

Scheme 2. Schematic Representation of the Synthetic Routes to the Tungsten Complexes and Labeling Scheme for These

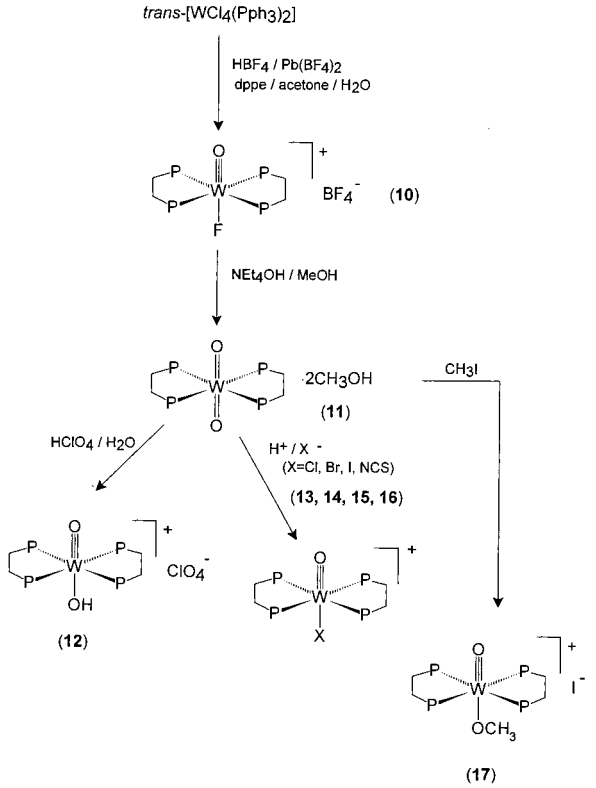

complex as the only reactive species, has been established for the substitution reactions of *trans*-dioxo tetracyano complexes of Mo(IV), W(IV), Re(V), and Tc(V)[28] and of *trans*-$[Os(N)(H_2O)(CN)_4]^-$.[29]

On the other hand is the difference in reactivity between the dioxo and the hydroxo-oxo complexes notable. The former species thus react with neat $(CH_3)_3SiCl$ within seconds at room temperature to give the *trans*-$[M(O)(Cl)(dppe)_2]Cl$ (M = Mo, W) compounds in quantitative yield, whereas 2 h at room temperature in neat $(CH_3)_3SiCl$ leave the hydroxo complexes unchanged.

UV−Vis Spectroscopy. For systems with d^2 electronic configuration, Figure 1 lead us to expect transitions with the following symmetries, orbital character, and energetic ordering: $^1A_1(C_{4v}) \rightarrow {}^3E(C_{4v})$ ($d_{xy}^2 \rightarrow d_{xy}$, $\{d_{yz}, d_{zx}\}$), $^1A_1(C_{4v}) \rightarrow {}^1E(C_{4v})$ ($d_{xy}^2 \rightarrow d_{xy}$, $\{d_{yz}, d_{zx}\}$), $^1A_1(C_{4v}) \rightarrow {}^3A_2(C_{4v})$ ($d_{xy}^2 \rightarrow d_{xy}$, $d_{x^2-y^2}$), and $^1A_1(C_{4v}) \rightarrow {}^1A_2(C_{4v})$ ($d_{xy}^2 \rightarrow d_{xy}$, $d_{x^2-y^2}$). The most significant difference between the transitions to states with E-symmetry to states with A_2 symmetry, respectively, is their dependence on the ligation sphere. The transition to $^{1,3}E$ states promotes an electron from the nonbonding d_{xy} orbital to the degenerate set $\{d_{yz}, d_{zx}\}$ which has π-symmetry with respect to the axial ligands. This transition is therefore expected to depend on the nature of the ligand trans to the oxo ligand directly as well as through its influence on the oxo-ligand. The transitions to the $^{1,3}A_2$ states on the other hand involve shifting an electron to the $d_{x^2-y^2}$ orbital, which σ- and π-interacts only with the equatorial phosphine ligands. These transitions should thus be independent of the nature of the axial ligands.

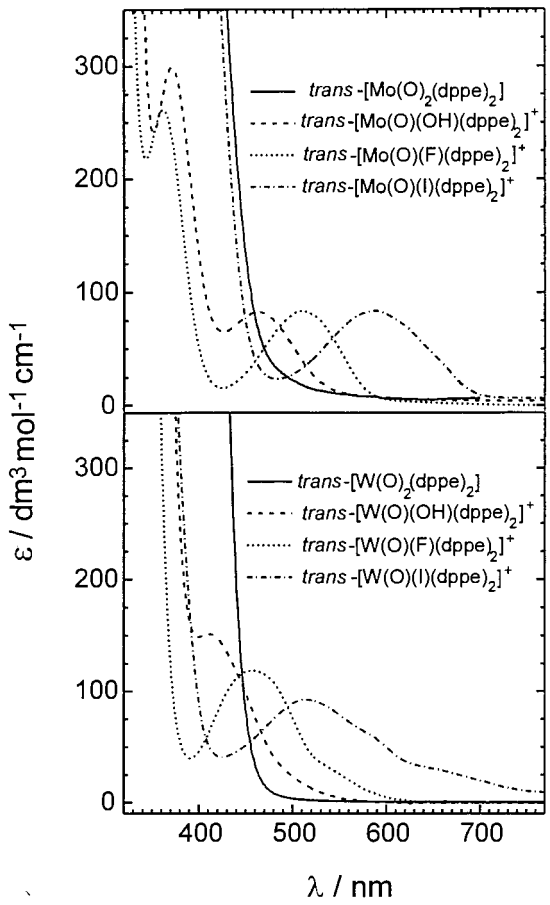

Figure 2. Electronic absorption spectra of *trans*-$[M(O)_2(dppe)_2]$ and *trans*-$[M(O)(X)(dppe)_2]^+$ (X = OH, F, I; M = Mo (top), W (bottom)). All spectra were recorded in $CHCl_3$; cf. Table 2 for spectral characteristics.

In Figure 2 the UV−vis spectra of the *trans*-$[M(O)(X)(dppe)_2]^{0/+}$ species for X = O, OH, F, and I are shown for comparison. The remaining spectral data are summarized in Table 2. As for the molybdenum analogue,[12] we observe no bands in the spectrum of **11** with wavelengths above 400 nm. The spectrum of this complex was recorded immediately after dissolving the compound. This is necessary since the compound reacts fast with halogenated organic solvents to produce solutions with distinctly different spectra. The featureless spectrum of **11** contains no information regarding the energetic ordering of the metal d^2 states. For the mono-oxo species the pronounced dependence of the position of the lowest energy band on the nature of the axial ligands proves this transition to be of $d_{xy} \rightarrow \{d_{yz}, d_{zx}\}$ character.

Importantly, the intensity of the band or band system with lowest energy is very similar for the two metals. If the transitions were spin forbidden, their intensity should be proportional to the square of the spin−orbit coupling parameter. Since the spin−orbit coupling parameters for gaseous Mo(IV) and W(IV) are 920 and 3100 cm^{-1}, respectively,[30] it can be concluded that the observed bands of lowest energy with molar extinction coefficients in the range 50−150 $dm^3\ mol^{-1}\ cm^{-1}$ are spin allowed ($^1A_1 \rightarrow {}^1E$).

The data in Table 2 encompasses seven pairs of analogous tungsten and molybdenum where the $^1A_1 \rightarrow {}^1E$ transition has

(28) (a) Roodt, A.; Leipoldt, J. G.; Helm, L.; Merbach, A. E. *Inorg. Chem.* **1994**, *33*, 140. (b) Leipoldt, J. G.; van Eldik, R.; Basson, S. S.; Roodt, A. *Inorg. Chem.* **1986**, *25*, 4639. (c) Leipoldt, J. G.; Basson, S. S.; Roodt, A.; Purcell, W. *Transition Met. Chem.* **1987**, *12*, 209.

(29) Van Der Westhuizen, H. J.; Basson, S. S.; Leipoldt, J. G.; Purcell, W. *Polyhedron* **1994**, *13*, 717.

(30) Bendix, J.; Brorson, M.; Schäffer, C. E. *Inorg. Chem.* **1993**, *32*, 2838.

Table 2. Spectroscopic Data for Complexes

complex	UV−vis λ/nm (ϵ/mol^{-1} dm^3 cm^{-1})	IR/Raman $\nu_{M=O}$/cm^{-1}	NMR $\delta(^{31}P)$/ppm
1	509 (83.7)	944 (IR)	39.8 (d, $^2J_{P-F}$ = 40.3 Hz)
	362 (262)		
2	−	808 (Raman)	34.9
3	461 (82.7)	897 (IR)	37.2
	371 (300) sh		
4	566 (64.9)	943 (IR)	40.3
5	573 (64.2)	942 (IR)	37.4
6	587 (83.8)	945 (IR)	32.8
7	589 (112)	945 (IR)	44.6
8	463 (107)	889 (IR)	37.6
	377 (324) sh		
9	572 (104)	933 (IR)	42.0
10	457 (119)	945 (IR)	31.7 ($^1J_{P-W}$ = 320 Hz) ($^2J_{P-F}$ = 45.1 Hz)
11	−	840 (Raman)	22.5 (s,d, $^1J_{P-W}$ = 328 Hz)
12	411 (151)	902 (IR)	27.0 (s,d, $^1J_{P-W}$ = 318 Hz)
13	502 (81.3)	952 (IR)	27.6 (s,d, $^1J_{P-W}$ = 314 Hz)
14	505 (90.3)	954 (IR)	23.8 (s,d, $^1J_{P-W}$ = 314 Hz)
15	517 (84.5)	952 (IR)	17.2 (s,d, $^1J_{P-W}$ = 314 Hz)
16	536 (73.3)	951 (IR)	32.5 (s,d, $^1J_{P-W}$ = 312 Hz)
17	416 (181)	892 (IR)	28.2 (s,d, $^1J_{P-W}$ = 318 Hz)

been observed. The ratios between the energy of the lowest absorption band maximum in these pairs of tungsten and molybdenum complexes fall within the narrow range 1.10−1.14. For octahedral systems the ratio between the spectrochemical parameters for 5d and 4d metals is generally higher: 1.2−1.3, but with much variation.[31] Our results are though in good agreement with the trends observed for the $^2B_2 \rightarrow {}^2E$ transition in tetragonal d^1 oxo-halide systems. This transition energy is determined only by π-bonding effects and varies little across and down the periodic table. The energy of this transition increases by a factor of 1.10−1.15 [sic] upon going from one period to the next.[1]

The spectra of the tungsten species all show a first absorption band with distinct structure. Since the ^1E state cannot be split by spin−orbit coupling, we conclude that the structure is due to spin−orbit coupling mixing of the ^1E and ^3E states. The energy difference between these states is expected to be similar for the molybdenum and tungsten species since interelectronic repulsion parameters generally are very similar for corresponding $4d^q$ and $5d^q$ systems.[32] This together with the much higher value of the spin−orbit coupling parameter increases the intermixing of the ^1E and ^3E states in the tungsten complexes. The low-energy, lower intensity components of these composite bands are calculated to be predominantly ^3E and the component with highest energy to be predominantly ^1E. It is noteworthy that in the spectrum of *trans*-$[Mo(O)(I)(dppe)_2]^+$, but not in the spectra of any of the other molybdenum complexes, there is a clear asymmetry of the absorption band. This supports the suggestion that spin−orbit coupling is responsible for the shape of the tungsten spectra. Other examples are known where transition metal iodo-complexes, such as $[Cr(NH_3)_5I]^{2+}$, show large spin−orbit coupling effects in formally metal centered states.[33]

In the spectra of $[Mo(O)(F)(dppe)_2]^+$ and $[Mo(O)(OH)(dppe)_2]^+$ a second absorption band is observed. The energy

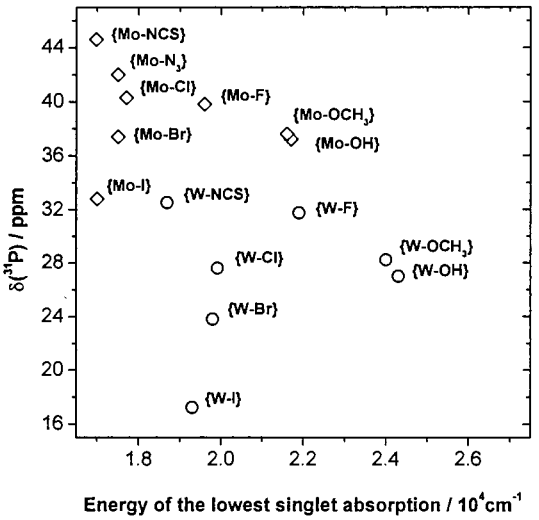

Figure 3. Plot showing the correspondence between the energy of the first band maximum in the absorption spectrum and the chemical shift of the phosphorus nuclei. The complexes have been abbreviated by the metal and the *trans*-to-oxygen ligand.

of this absorption is quite similar for the two systems suggesting, in accordance with the scheme in Figure 1, the transition to have the orbital character $d_{xy}^2 \rightarrow d_{xy}, d_{x^2-y^2}$. The intensity of this absorption band when compared to that of the spin-allowed bands assigned above makes us assign it to the transition $^1A_1 \rightarrow {}^1A_2$.

By dissolving salts of the *trans*-$[M(O)(OH)(dppe)_2]^+$ ions in acetone and adding excess of neat CF_3SO_3H, blue solutions with red shifted spectra compared to the hydroxo species were obtained (Mo, 587 nm, 85.0 mol^{-1} dm^3 cm^{-1}; W, 521 nm, 79.1 mol^{-1} dm^3 cm^{-1}). The blue species produced are believed to be the *trans*-$[M(O)(H_2O)(dppe)_2]^{2+}$ ions. The oxo-aqua formulation is in line with the known[34] behavior of the cyanide complexes. However, the tautomeric di-hydroxo formulation cannot be ruled out, as shown by the fact that the isoelectronic *trans*-$[Mo(NH)(OH)(dppe)_2]^+$ upon protonation crystallizes as a salt of the *trans*-$[Mo(NH_2)(OH)(dppe)_2]^{2+}$ ion.[35] The shifting of the absorption spectrum is in accordance with a the quoted assignment and a decreasing π-donor strength along the series $O^{2-} > OH^- > H_2O$.

^{31}P{^{1}H} NMR Spectroscopy. ^{31}P NMR shifts of the complexes have been summarized in Table 2. In the spectra of the molybdenum species only a single resonance is observed except for the fluoro complex (**1**) where it is split into a doublet due to coupling to the fluorine nucleus ($^2J_{P-F}$ = 40.3 Hz). In the tungsten complexes singlets with sidebands due to coupling to the ^{183}W nuclei ($I = {}^1/_2$, 14.27%) are observed. The $^1J_{P-W}$ values range from 312 to 328 Hz, which is in the range reported for similar systems.[36] In the spectrum of **10** these three lines are further split into doublets by a smaller coupling (45.1 Hz) to the fluorine nucleus.

It is a noteworthy common feature of the hitherto described *trans*-dioxo molybdenum and tungsten complexes that they in addition to the strong axial π-donors have typical π-acceptors as auxiliary equatorial ligands. The coexistence of ligands,

(31) Lever, A. B. P. *Inorganic Electronic Spectroscopy*; Elsevier: Amsterdam, 1984.
(32) For Rh(III) and Ir(III), see: Jørgensen, C. K. *Modern Aspects of Ligand Field Theory*; North-Holland: Amsterdam, 1971. For the d^2 systems Nb(III) and Ta(III), see: Brorson, M.; Schäffer, C. E. *Inorg. Chem.* **1988**, *27*, 2522.
(33) Pedersen, E.; Toftlund, H. *Inorg. Chem.* **1974**, *13*, 1603.
(34) (a) Robinson, P. R.; Schlemper, E. O.; Murmann, R. K. *Inorg. Chem.* **1975**, *14*, 2035. (b) Smit, J. P.; Purcell, W.; Roodt, A.; Leipoldt, J. G. *Polyhedron* **1993**, *12*, 2271.
(35) Adachi, T.; Hughes, D. L.; Ibrahim, S. K.; Okamoyo, S.; Pickett, J.; Yabanouchi, N.; Yoshida, T. *J. Chem. Soc., Chem. Commun.* **1995**, 1081.
(36) Brevard, C.; Granger, P. *Handbook of High-Resolution Multinuclear NMR*; John Wiley: New York, 1981.

which normally are associated with different oxidation states, is facilitated by the geometry in these tetragonal systems where the equatorial π-acceptors are optimally arranged to relieve the π-electron density donated by the axial ligands. This combination of strong π-donors and π-acceptors continues to exist for group 7 and group 8 d^2 systems exemplified by systems such as *trans*-$[Re(O)_2(dppe)_2]^+$ [37] and *trans*-$[Os(O)_2(2,2'$-bipyridine$)_2]^{2+}$.[38] However, for these centers with their higher oxidation states +5 and +6, the prevalence of back-bonding equatorial ligands ceases to be the rule and π-donating equatorial ligands, like OH^- and Cl^-, are also found.

It would be interesting to examine if this coexistence of ligands which normally stabilize widely different oxidation states can be ascribed to inter ligand π-bonding synergy. To try to illuminate this question we have plotted in Figure 3 the chemical shifts of the coordinated phosphines versus the energy of the first maximum in the absorption spectra. Representing the data in that way exhibits a high resemblance between the distribution patterns of the Mo and the W complexes.

A π-bonding synergy between the axial ligands and the equatorial phosphines would be expected to result in negative correlation between $\delta(^{31}P)$ and the energy of the $^1A_1 \rightarrow {}^1E$ transition. Clearly the relation is more complicated than so. The data for each metal fall into two groups: On one hand those systems where the ligating atoms are second row elements, and on the other hand the heavier (Cl, Br, I) halide complexes. The former group exhibits a negative correlation whereas the chloro, bromo, and iodo complexes deviate increasingly, showing larger NMR shielding of the phosphorus nuclei than expected from the spectrally determined donor strength of the axial ligands. The grouping of thiocyanate with the second-row donor ligands suggests it to be N-bound in these complexes. This assessment is verified by the X-ray structural analysis of the tungsten complex (vide infra).

From the data it is clear that axial ligands from different rows of The Periodic Table causes very different shieldings of the phosphorus nuclei. This result is surprising in view of the data presented in a recent paper dealing with *trans*-biscalcogenide complexes of molybdenum(IV): *trans*-$[Mo(Q)_2(PP)_2]$ where PP is a bidentate phosphine and Q = O, S, Se, Te.[11] For these closely related systems it was found that there was essentially no dependence of the $\delta(^{31}P)$ on the axial ligands.

^{19}F NMR Spectroscopy. The fluoro complexes show ^{19}F NMR spectra which consist of 5 lines at −119.8 ppm (Mo) respectively seven lines at −136.1 ppm (W). From the ^{31}P NMR values for the coupling constants $^1J_{P-W} = 320$ Hz (^{183}W, $I = {}^1/_2$, 14.27%) and $^2J_{P-F} = 45.1$ Hz can be determined. The ^{19}F NMR spectrum of *trans*-$[W(O)(F)(dppe)_2](BF_4)$ consists of a seven-line pattern with apparently one coupling constant identical to the 45 Hz determined from the ^{31}P NMR spectrum. The seven-line spectrum is due to the ratio $^1J_{F-W}/^2J_{P-F}$ accidentally being very close to 2. This assessment can be verified by comparing the relative intensities of the lines in the seven-line pattern. Calculated and experimentally determined relative intensities are collected in Table 3. The measured and calculated relative intensities agree well and rule out the alternative possibility that the $^1J_{F-W}$ is a higher multiplum of the $^2J_{P-F}$ and some small lines are unobserved.

Vibrational Spectroscopy. The M═O stretching frequencies are collected in Table 2. The hydroxo and methoxo complexes have stretching frequencies between 889 and 902 cm^{-1}, which is distinctly lower than those in the halide and pseudo-halide complexes (933−952 cm^{-1}). This grouping is different from the UV−vis spectra where fluoride was found to be different from the other halides and intermediate between these and the hydroxide and methoxide. The data compares well with the literature data on similar complexes, e.g., $Na_3[Mo(O)(OH)(CN)_4]\cdot 4H_2O$ (937 cm^{-1}),[39] $[Mo(O)(Cl)(dppe)_2](BPh_4)$ (940 cm^{-1}),[40] and *trans*-$(NMe_4)_3[W(O)(NCS)(CN)_4]\cdot$NaNCS (954 cm^{-1}).[41] The symmetric Raman active stretch in the *trans*-dioxo complexes is found at 811 cm^{-1} (**2**) for molybdenum and 840 cm^{-1} (**11**) for tungsten. This is between those reported for $NaK_3[M(O)_2(CN)_4]\cdot 6H_2O$ (Mo, 783 cm^{-1}; W, 795 cm^{-1})[42] and $M(O)_2(CO)_4$ (Mo, 820 cm^{-1}; W, 850 cm^{-1}).[9] The ordering with higher $\nu_{O=M=O}$ symmetry for tungsten than for molybdenum is thus found for the neutral phosphine and the carbonyl complexes as well as for the tetraanionic cyano complexes indicating slightly stronger tungsten-oxo than molybdenum-oxo bonds.

Table 3. Calculated and Measured Intensities in the ^{19}F NMR Spectrum of *trans*-$[W(O)(F)(dppe)_2]^+$

relative intensity	
calcd	exptl
100.0	100.0
68.8	68.6/69.5
20.0	20.2/20.6
1.25	1.53/1.57

X-ray Crystallography. The molecular structures of the tungsten complexes **10**, **11**, **12**, and **16** have been determined from single-crystal X-ray diffraction. The structures are shown in Figures 4−7. Selected bond lengths and angles are listed in Tables 4−7. Complete structural data are available in the Supporting Information. The structures are similar, based on octahedral coordination of the tungsten, with the phosphine ligators coordinating in the equatorial plane and the oxo and auxiliary ligand situated trans to each other. The preference for a trans arrangement of two π-donor ligands in systems with d^2 electronic configuration has been thoroughly discussed.[43]

trans-$[W(O)_2(dppe)_2]\cdot 2CH_3OH$ (**11**) is the first structurally characterized dioxo−W(IV) complex. It is isomorphous with the analogous molybdenum complex (**2**)[12] crystallizing in the triclinic space group $P\bar{1}$ with the tungsten atom situated on a center of inversion. The tungsten−oxygen bond length of 1.8298(11) Å is a little, but significantly, longer than the 1.8183(8) Å found for the Mo−O bond length in *trans*-$[Mo(O)_2(dppe)_2]\cdot 2CH_3OH$. Conversely, the metal−phosphorus bond lengths are 0.010(1) Å shorter in the tungsten complex than in the molybdenum analogue. In isoelectronic *trans*-$[Re(O)_2(dppe)_2]^+$ [44] the rhenium-oxo bond length is 1.781(6) Å and the average Re−P bond length is 2.491(3) Å almost identical to that in **11**.

The tungsten-oxo bond lengths show the expected large dependence on the trans ligand: 1.8298(11) Å (**11**), 1.7610(14)

(37) Meyer, K. E.; Root, D. R.; Fanwick, P. E.; Walton, R. R. *Inorg. Chem.* **1992**, *31*, 3067.
(38) Dobson, J. C.; Takeuchi, K. J.; Pipes, D. W.; Geselowitz, D. A.; Meyer, T. J. *Inorg. Chem.* **1986**, *25*, 2357.
(39) Dudek, M.; Kanas, A.; Samotus, A. *J. Inorg. Nucl. Chem.* **1979**, *41*, 1135.
(40) Levason, W.; McAuliffe, C. A.; Sayle, B. J. *J. Chem. Soc., Dalton Trans.* **1976**, 1177.
(41) Roodt, A.; Leipoldt, J. G.; Basson, S. S.; Potgeiter, I. M. *Transition Met. Chem.* **1990**, *15*, 439.
(42) Dudek, M.; Kanas, A.; Samotus, A. *J. Inorg. Nucl. Chem.* **1980**, *42*, 1701.
(43) (a) Mingos, D. M. P. *J. Organomet. Chem.* **1979**, *179*, C29. (b) Demachy, I.; Jean, Y. *Inorg. Chem.* **1997**, *36*, 5956 and references therein.
(44) Meyer, K. E.; Root, D. R.; Fanwick, P. E.; Walton, R. A. *Inorg. Chem.* **1992**, *31*, 3067.

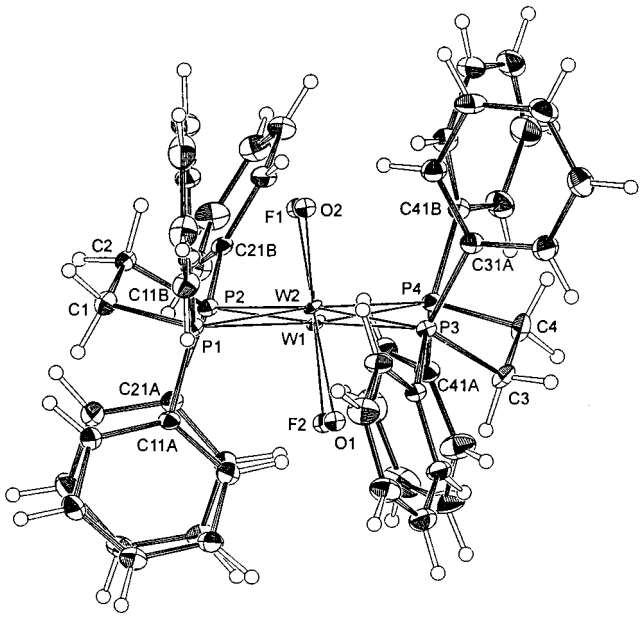

Figure 4. ORTEP-II drawing and atom-numbering scheme of the cation in **10**. Displacement ellipsoids are drawn at the 50% probability level. Hydrogen atoms are shown as spheres of arbitrary size. Both of the two almost equally populated independent O−W−F fragments are shown.

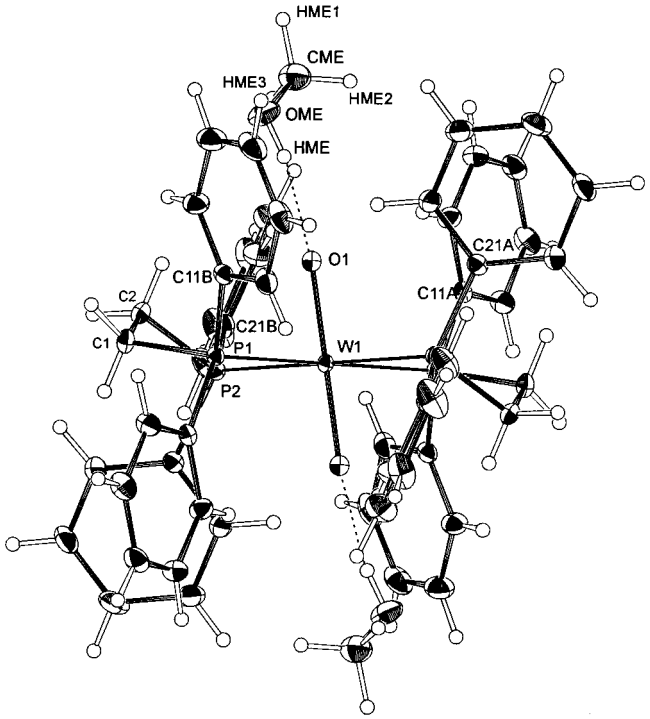

Figure 5. ORTEP-II drawing and labeling scheme of the molecular structure of **11**. Displacement ellipsoids are drawn at the 50% probability level. Hydrogen atoms are shown as spheres of arbitrary size.

Å (**12**), 1.721(5) Å (**16**), and 1.718(9) Å (**10**). As discussed by Cotton *et al.*[11] the maximal bond order in the centrosymmetric dioxo complex is two for symmetry reasons. With decreasing *trans*-influence exerted upon the oxo-ligand the bond order approaches three in the fluoride and isothiocyanate complexes. An even shorter W^{IV}−O bond length of 1.687(7) Å has been found in *trans*-$[W(O)(Cl)(dppe)_2]^+$.[16]

The structure of **16** confirms that the thiocyanate is N-bonded. A conclusion also reached from the data point distribution in

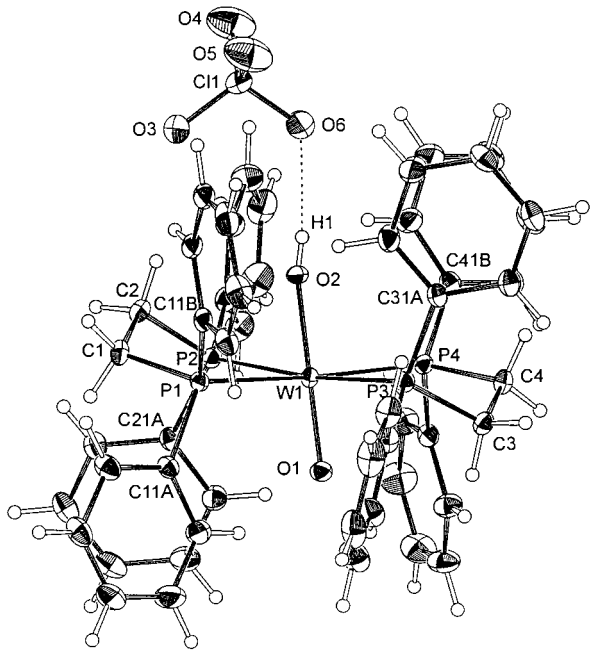

Figure 6. ORTEP-II drawing and atom-numbering scheme of **12**. Displacement ellipsoids are drawn at the 50% probability level. Hydrogen atoms are shown as spheres of arbitrary size.

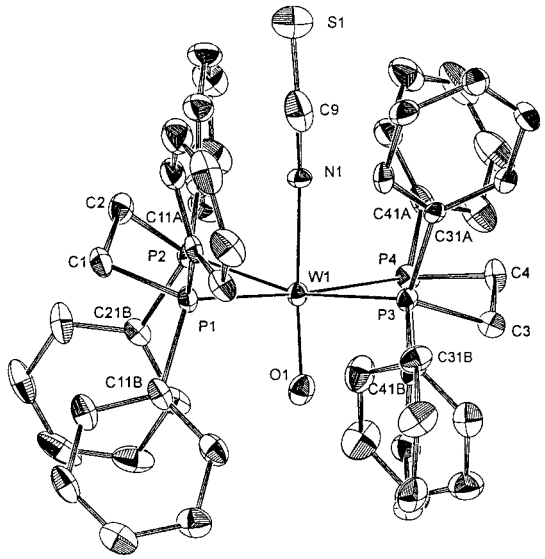

Figure 7. ORTEP-II drawing and atom-numbering scheme of the cation in **16**. Displacement ellipsoids are drawn at the 50% probability level. Hydrogen atoms are shown as spheres of arbitrary size.

Figure 3. The W−N bond length is 2.104(5) Å. This is significantly shorter than the value (2.23(2) Å) found in $(NMe_4)_3$-$[W(O)(NCS)(CN)_4]\cdot NaNCS$,[41] but in the range (2.090−2.205 Å) found in $[W_3S_4(NCS)_9]^{5-}$.[45]

The variations in the tungsten phosphorus bond lengths, albeit small, are in accordance with the notion of inter ligand π-bonding synergy. The average W−P bond length thus increases along the series **11** (2.500 Å), **12** (2.521 Å), **10** (2.53 Å), and **16** (2.53 Å) contrary to what is expected from charge considerations. The same ordering is found for the molybdenum compounds **2** (2.510 Å),[12] **3** (2.536 Å),[46] and **1** (2.54 Å).[47]

(45) Shibahara, T.; Kohda, K.; Ohtsuji, A.; Yasuda, K.; Kuroya, H. *J. Am. Chem. Soc.* **1986**, *108*, 2757.
(46) Bendix, J.; Bøgevig, A. *Acta Crystallogr. (C)* **1998**, *54*, 206.
(47) Bendix, J.; Bøgevig, A. Unpublished results.

Table 4. Selected Bond Lengths [Å] and Angles [deg] for *trans*-[W(O)(F)(dppe)$_2$](BF$_4$) (**10**)[a]

W(1)−O(1)	1.718(9)	W(2)−O(2)	1.718(9)
W(1)−F(1)	2.001(7)	W(2)−F(2)	2.001(7)
W(1)−P(3)	2.512(2)	W(2)−P(2)	2.508(2)
W(1)−P(4)	2.5195(17)	W(2)−P(1)	2.5186(18)
W(1)−P(2)	2.522(2)	W(2)−P(3)	2.544(2)
W(1)−P(1)	2.5582(17)	W(2)−P(4)	2.5586(18)
O(1)−W(1)−F(1)	178.1(4)	O(2)−W(2)−F(2)	178.3(6)
O(1)−W(1)−P(3)	82.6(5)	O(2)−W(2)−P(2)	92.1(5)
F(1)−W(1)−P(3)	95.6(3)	F(2)−W(2)−P(2)	89.5(3)
O(1)−W(1)−P(4)	87.5(4)	O(2)−W(2)−P(1)	91.1(5)
F(1)−W(1)−P(4)	91.9(4)	F(2)−W(2)−P(1)	89.1(3)
P(3)−W(1)−P(4)	79.76(5)	P(2)−W(2)−P(1)	79.63(5)
O(1)−W(1)−P(2)	100.6(5)	O(2)−W(2)−P(3)	97.6(5)
F(1)−W(1)−P(2)	81.3(3)	F(2)−W(2)−P(3)	80.7(3)
P(3)−W(1)−P(2)	176.35(9)	P(2)−W(2)−P(3)	169.83(9)
P(4)−W(1)−P(2)	98.44(7)	P(1)−W(2)−P(3)	103.04(7)
O(1)−W(1)−P(1)	99.2(4)	O(2)−W(2)−P(4)	95.3(5)
F(1)−W(1)−P(1)	81.5(4)	F(2)−W(2)−P(4)	84.6(3)
P(3)−W(1)−P(1)	102.82(7)	P(2)−W(2)−P(4)	97.80(7)
P(4)−W(1)−P(1)	173.05(10)	P(1)−W(2)−P(4)	173.24(9)
P(2)−W(1)−P(1)	78.61(5)	P(3)−W(2)−P(4)	78.43(5)

[a] O(2), W(2), and F(2) belong to the second oppositely oriented fragment introduced to describe the disorder of these atoms.

Table 5. Selected Bond Lengths [Å] and Angles [deg] for *trans*-[W(O)$_2$(dppe)$_2$]·2CH$_3$OH (**11**)[a]

W−O(1)	1.8298(11)
W−P(2)	2.4955(7)
W−P(1)	2.5065(12)
O(1)−W−O(1)^i	180.0
O(1)−W−P(2)	84.10(4)
O(1)^i−W−P(2)	95.90(4)
O(1)−W−P(1)	84.40(4)
O(1)^i−W−P(1)	95.60(4)
P(2)−W−P(1)	79.49(3)
P(2)^i−W−P(1)	100.51(3)

[a] Symmetry transformations used to generate equivalent atoms: (i) $-x, -y, -z$.

Table 6. Selected Bond Lengths [Å] and Angles [deg] for *trans*-[W(O)(OH)(dppe)$_2$](ClO$_4$) (**12**)

W(1)−O(1)	1.7610(14)	W(1)−P(1)	2.5182(6)
W(1)−O(2)	1.9157(14)	W(1)−P(2)	2.5212(8)
W(1)−P(3)	2.5137(8)	W(1)−P(4)	2.5292(7)
O(1)−W(1)−O(2)	179.29(6)	P(3)−W(1)−P(2)	173.220(16)
O(1)−W(1)−P(3)	87.39(5)	P(1)−W(1)−P(2)	79.077(19)
O(2)−W(1)−P(3)	93.08(5)	O(1)−W(1)−P(4)	86.58(5)
O(1)−W(1)−P(1)	96.57(5)	O(2)−W(1)−P(4)	92.98(5)
O(2)−W(1)−P(1)	83.89(5)	P(3)−W(1)−P(4)	79.509(19)
P(3)−W(1)−P(1)	98.535(19)	P(1)−W(1)−P(4)	176.240(15)
O(1)−W(1)−P(2)	99.16(5)	P(2)−W(1)−P(4)	102.502(19)
O(2)−W(1)−P(2)	80.39(5)		

In **11** a methanol molecule is hydrogen bonded to each of the terminal oxo-ligands (Figure 5). The bridging hydrogen atom was located in the electron density map and its position refined. The distance between the donor (OME) and the acceptor (O1) is 2.710 Å, rendering it a medium strength hydrogen bond on distance-based criteria.[48] In **12**, a hydrogen bond between the hydroxo ligand in the cation and the perchlorate counterion (Figure 6) prevents the type of disorder found in **10**. The arrangement is similar to that found in the analogous Mo compound.[46] The hydrogen bond (O6···H1−O2) is a little longer (2.769(3) Å) than that found in the dioxo complex, but like the latter it is nearly linear (169(5)°).

Table 7. Selected Bond Lengths [Å] and Angles [deg] for *trans*-[W(O)(NCS)(dppe)$_2$](BPh$_4$) (**16**)

W(1)−O(1)	1.721(5)	W(1)−P(1)	2.536(2)
W(1)−N(1)	2.104(5)	W(1)−P(4)	2.541(2)
W(1)−P(2)	2.527(2)	N(1)−C(9)	1.184(13)
W(1)−P(3)	2.536(2)	C(9)−S(1)	1.593(13)
O(1)−W(1)−N(1)	177.1(3)	P(3)−W(1)−P(1)	100.58(8)
O(1)−W(1)−P(2)	102.4(2)	O(1)−W(1)−P(4)	89.1(2)
N(1)−W(1)−P(2)	80.5(2)	N(1)−W(1)−P(4)	90.5(2)
O(1)−W(1)−P(3)	91.6(2)	P(2)−W(1)−P(4)	100.47(8)
N(1)−W(1)−P(3)	85.5(2)	P(3)−W(1)−P(4)	79.78(8)
P(2)−W(1)−P(3)	166.00(7)	P(1)−W(1)−P(4)	175.95(8)
O(1)−W(1)−P(1)	94.9(2)	C(9)−N(1)−W(1)	178.8(8)
N(1)−W(1)−P(1)	85.5(2)	N(1)−C(9)−S(1)	175.8(11)
P(2)−W(1)−P(1)	78.19(8)		

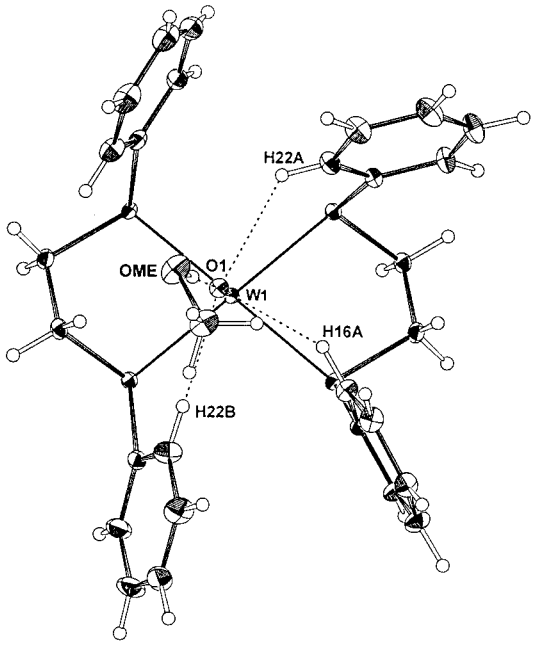

Figure 8. Top view of *trans*-[W(O)$_2$(dppe)$_2$]·2CH$_3$OH (**11**) showing the interactions between the terminal oxo ligand and hydrogen atoms from three phenyl groups and the hydrogen bond to the methanol adduct molecule. The molecule lies on a center of inversion. Only one-half of the molecule is shown.

Except for the *trans*-dioxo compound where the tungsten atom lies on an inversion center, the tungsten atom is raised out of the plane spanned by the four equatorial phosphorus ligators toward the oxo-ligand. This type of distortion is common in octahedral systems with one strong π-donor. For six-coordinate systems the out-of-plane distance is generally in the range 0.05−0.30 Å.[1] In five-coordinate complexes the metal out-of-plane displacement is generally larger with the 0.82 Å in [(AsPh$_4$)-Mo(O)(SPh)$_4$] representing the high end.[49] This pattern of parallel variation of the out-of-plane displacement and the asymmetry in the donor strength of the axial ligators is also found in the complexes in this study. The out-of-plane displacements are 0.1069(3) Å (**12**), 0.107(2)/0.178(2) Å (**10**), and 0.198(4) Å (**16**), respectively, for the three mono cations. Often this type of deviation from orthoaxiality is discussed in terms of the angle between the multiple-donor and the *cis*-ligands. However, in the present context this measure loses it importance due to fairly large tilt of the metal-oxo axis with

(48) Jeffrey, G. A. *An Introduction to Hydrogen Bonding*; Oxford University Press: New York, 1997.
(49) Bradbury, J. R.; Mackay, M. F.; Wedd, A. G. *Aust. J. Chem.* **1978**, *31*, 2423.
(50) Levason, W.; Champness, N. R.; Webster, N. *Acta Crystallogr. (C)* **1993**, *49*, 1884.

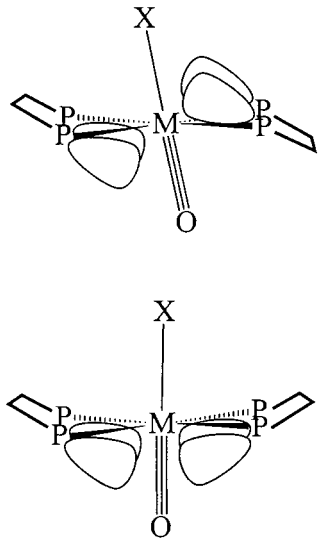

Figure 9. Illustration of the influence of the phosphine backbone orientations on the angle between the P_4 plane and the π-donor axis.

respect to the plane spanned by the four equatorial phosphorus donors. The angle between M═O axis and the P_4 plane is 82.51(5)° (**11**), 82.87(5)° (**12**), 83.3(4)° (average) (**10**), and 84.5(2)° (average) (**16**), respectively. In *trans*-$[Re(O)_2(dppe)_2](ReO_4)$ a similar angle (83.4°) between the Re═O axis and the P_4 plane is found.[48]

When Figures 4−7 are examined, it is seen that there are close contacts between hydrogen atoms from four to six of the phenyl groups and the electronegative axial ligands (cf. Figure 8). The contacts are in the range 2.25−2.8 Å, which corresponds to accepted values for C−H···O hydrogen bonds.[48] It is however peculiar how the hydrogen bond acceptor is bent away to accommodate this quite weak interaction. An examination of all structurally characterized *trans*-bis complexes of bidentate phosphine and arsine complexes revealed the tilt between the axial ligands and the P_4/As_4 plane to be a quite general property. It is not only found for axial ligands which are good hydrogen bond acceptors, but also in complexes such as *trans*-$[OsCl_2(dppe)_2]$ (82.10°)[50] and *trans*-$[Mo(N_2)_2(dppe)_2]$ (84.55°).[51] On the other hand the tilt is absent in some complexes with good hydrogen bond accepting axial ligands such as in *trans*-$[Mo(O)(S)(dppee)_2]$ (89.08°/88.51°).[11] We have found that the complete body of structural data can be rationalized by a repulsive interaction between the donated electron density from the phosphine (arsine) ligands and the electron density in the bonds to the axial ligands. A schematic representation of this model is given in Figure 9, which shows how the backbone conformation of the phosphine ligands is crucial in determining the tilt. A full account these results will be presented elsewhere. In summary, the contacts between the hydrogen atoms from the phenyl groups and the axial ligands are facilitated by the tilting of the axial ligands with respect to the P_4 plane, but not the cause of it.

(51) Uchida, T.; Uchida, Y.; Hidai, M.; Kodama, T. *Acta Crystallogr. (B)* **1975**, *31*, 1997.

Conclusions

The synthesis and acid-catalyzed substitution reactions of *trans*-$[W(O)_2(dppe)_2]\cdot 2CH_3OH$ has shown tungsten to have a chemistry that closely parallels that of molybdenum in compounds of this type. These neutral complexes are versatile starting materials for mono-oxo complexes. Their full potential in this respect is not exhausted by the compounds described here. Both ^{31}P NMR and UV−vis spectrochemical parameters show completely identical dependence on the auxiliary ligand for molybdenum and tungsten. The dependence of the ^{31}P chemical shifts on the nature of the axial ligands is significant and can be taken as evidence for π-bonding synergy between π-donor and -acceptor ligands. The data for the metal−phosphorus bond lengths corroborate the existence of such a synergy. From the electronic spectra identical π-spectrochemical series for the two metals could be deduced: $O^{2-} > OH^- \approx CH_3O^- > F^- > Cl^- \approx Br^- > I^- > NCS^-$. The magnitude of energy splittings determined mainly by π-bonding effects increases by a factor of 1.10−1.14 upon going from Mo(IV) to W(IV).

Acknowledgment. We thank Prof. C. E. Schäffer and Prof. S. Larsen for valuable discussions. Mr. F. Hansen and Mrs. H.K. Andersen are thanked for valuable technical assistance. We thank Mr. A. Goebbls for measuring the magnetic susceptibilities.

Supporting Information Available: Complete X-ray crystallographic files in CIF format are available on the Internet only. FAB^+ mass spectra of all new complexes, magnetic susceptibility data for *trans*-$[M(O)(F)(dppe)_2](BF_4)$ (M = Mo, W), and details of the structure determinations (9 pages). Ordering information is given on any current masthead page.

IC980342U